Life of a Six-Hour Hurricane

Kay L. Shelton and John Molinari

Department of Earth and Atmospheric Sciences, University at Albany, State University of New York, Albany, New York

(Manuscript received 30 November 2007, in final form 20 June 2008)

ABSTRACT

Hurricane Claudette developed from a weak vortex in 6 h as deep convection shifted from downshear into the vortex center, despite ambient vertical wind shear exceeding 10 m s^{-1}. Six hours later it weakened to a tropical storm, and 12 h after the hurricane stage a circulation center could not be found at 850 hPa by aircraft reconnaissance. At hurricane strength the vortex contained classic structure seen in intensifying hurricanes, with the exception of 7°–12°C dewpoint depressions in the lower troposphere upshear of the center. These extended from the 100-km radius to immediately adjacent to the eyewall, where equivalent potential temperature gradients reached 6 K km^{-1}. The dry air was not present prior to intensification, suggesting that it was associated with vertical shear–induced subsidence upshear of the developing storm. It is argued that weakening of the vortex was driven by cooling associated with the mixing of dry air into the core, and subsequent evaporation and cold downdrafts. Evidence suggests that this mixing might have been enhanced by eyewall instabilities after the period of rapid deepening. The existence of a fragile, small, but genuinely hurricane-strength vortex at the surface for 6 h presents difficult problems for forecasters. Such a "temporary hurricane" in strongly sheared flow might require a different warning protocol than longer-lasting hurricane vortices in weaker shear.

1. Introduction

Predicting the intensity of a tropical cyclone that exists within a sheared environment remains a problem for hurricane forecasters. Through both observational studies (e.g., Reasor et al. 2000; Black et al. 2002; Corbosiero and Molinari 2002; Chen et al. 2006) and numerical modeling studies (e.g., Frank and Ritchie 2001; Rogers et al. 2003; Braun et al. 2006; Braun and Wu 2007) it has been shown that vertical wind shear projects a wavenumber 1 azimuthal asymmetry on the vertical motion and precipitation fields in tropical cyclones. In general, enhanced ascent (and hence convection) is favored downshear, associated with the secondary circulation that maintains balance in response to the shear-tilted vortex; descent is favored on the upshear side of the vortex.

For the most part, research has shown that shear has a negative influence on the intensity of tropical cyclones (e.g., Frank and Ritchie 2001; Black et al. 2002; Wong and Chan 2004), with even mature hurricanes weakening when exposed to strong (>10 m s^{-1}) vertical wind shear. However, some examples of storms developing or intensifying in the presence of strong shear have been found. Davis and Bosart (2003) investigated the role of vertical wind shear in the transition of subtropical cyclones into full tropical cyclones. In every case, vertical wind shear decreased prior to development as a result of potential vorticity redistribution by convection and convectively induced outflow. The convection was generated in association with vertical motions driven by the initial baroclinic system. Davis and Bosart (2004) labeled this process "tropical transition." This provides one path by which a tropical cyclone can develop in the presence of large vertical wind shear.

Molinari et al. (2004, 2006) investigated weak systems that intensified in the presence of strong vertical wind shear (10–15 m s^{-1}). In both cases, a strong vortex developed within downshear convection. The new mesoscale vortex interacted with, and appeared to absorb, the original vortex in a manner similar to the modeling studies of Enagonio and Montgomery (2001). The resulting vortex was found to be stronger than the origi-

Corresponding author address: Kay L. Shelton, Department of Earth and Atmospheric Sciences, University at Albany, SUNY, 1400 Washington Ave., Albany, NY 12222.
E-mail: kay@atmos.albany.edu

DOI: 10.1175/2008MWR2472.1

nal vortex in both cases. Molinari et al. (2004, 2006) concluded that the vertical wind shear had contributed positively to the intensification of the systems. This statement does not necessarily imply that the influence of the shear resulted in a more rapid intensification than might have occurred without shear. Rather, vertical wind shear played an essential role in *how* the storms developed.

Hurricane Claudette (2003) provided an extreme example of intensification in the presence of large vertical wind shear. A hurricane-strength disturbance developed in less than 6 h while 850–200-hPa vertical wind shear exceeded 10 m s^{-1}. This hurricane then decayed in less than 6 h to a weak tropical storm. Claudette did not reach hurricane strength again for 4 days. In this paper, we will examine the growth and decay of this 6-h hurricane. This study makes extensive use of reconnaissance data collected by the U.S. Air Force Reserve (USAF) to analyze the evolution of Claudette. Although these data contain high temporal and spatial resolution, analysis is limited by the availability of just two flight levels of data, and usually only one level at a time. Supplementation with dropsonde data, when available, somewhat offsets this limitation.

2. Data sources

a. Flight-level data

The USAF provides estimates of the storm-center location and measurements of wind, temperature, dewpoint, and D value (radar altitude minus pressure altitude). A "figure-four" flight pattern is used, with radial flight legs extending ~200 km from the storm center. This flight pattern allows sampling in each quadrant of the storm at least once, and two estimates of the minimum central pressure and center location. Occasionally, this flight pattern is altered, most notably when the aircraft crew have trouble locating a circulation center (e.g., during the early stages of storm development). In this paper, observations from USAF flights at 850 and 700 hPa are used to show the thermodynamic and kinematic structure of the storm. When these observations are shown in the form of time series through the storm center, only those observations from approximately linear sections of the flight track are included. Due to small variations in the aircraft flight track (i.e., deviations from a straight line through the storm center), time, and radius do not have a strict one-to-one relationship. Therefore flight tracks are labeled using time rather than radius. Radius values for important points like the radius of maximum winds are provided. The National Oceanographic and Atmospheric Administration (NOAA) Hurricane Research Division (HRD) aircraft did not sample the storm during the period of interest.

The instruments aboard the USAF C-130H aircraft observe variables at a frequency of 1 Hz, and these observations are recorded at 0.1 Hz (a 10-s average). The data are processed in real time to identify potential errors. This processing includes 1) applying a coded flag to data points that could be erroneous in one or more variables, and 2) removing any occurrences of supersaturation by reducing the dewpoint to the temperature (Lt. Col. R. Henning 2004, personal communication). No further postprocessing is done to the archived data, except to ensure all the data are in chronological order.

The adjustment of the dewpoint temperature is applied to correct for supersaturation caused by sensor wetting (Eastin et al. 2002). By far the most common data flag used by the USAF identifies three variables (pressure altitude, dewpoint temperature, and wind direction) as possibly being in error. Of these three variables, a dewpoint temperature error is most likely. Shelton (2005) analyzed USAF reconnaissance data from 77 tropical cyclones (a total of 619 flights) from 1995 to 2003. The results of the study revealed the number of observations flagged by the USAF at the 850- and 700-hPa flight levels to be 2.9% and 4.5%, respectively. M. D. Eastin (2004, personal communication) found the number of observations in the HRD dataset in error due to sensor wetting at the 850- and 700-hPa flight levels to be 3.2% and 5.6%, respectively. Based on this, it is assumed that flagged points in the USAF data represent wetting errors. In this study, the flagged observations are retained and included in the data plots. However, where the flagged observations meet the criteria used by Eastin et al. (2002) to identify instrument wetting events, they will be marked by a shaded region. It will be seen that the conclusions of this study are not influenced by these sensor-wetting errors.

The USAF rarely samples storms at multiple flight levels during the same flight, precluding any rigorous analysis of the vertical structure of the storm. A simple equation will be derived to estimate the difference in storm intensity at an upper level given a horizontal temperature field at a lower level. The hypsometric (thickness) equation,

$$H = [(R/g)\overline{T}]\ln\left(\frac{p_1}{p_2}\right),$$

where $p_1 > p_2$, relates the mean temperature ($\overline{T}$) of a layer to its thickness (H). If the vertical lapse rate is

TABLE 1. Storm center locations for the reconnaissance center fixes and interpolated NHC best-track (BT) positions, and the difference between the two tracks. Where no location is given for the reconnaissance center fix, BT center locations are used.

Time and date	Reconnaissance center fix Lat (°)	Reconnaissance center fix Lon (°)	Interpolated BT center Lat (°)	Interpolated BT center Lon (°)	Center location difference (km)
0600 UTC 10 Jul	—	—	16.60	−81.70	—
1201 UTC 10 Jul	17.48	−82.75	17.50	−82.80	5.75
1352 UTC 10 Jul	17.70	−83.08	17.84	−83.20	20.09
1526 UTC 10 Jul	18.00	−83.27	18.13	−83.54	31.99
1706 UTC 10 Jul	18.20	−83.62	18.43	−83.90	39.09
2357 UTC 10 Jul	19.55	−85.53	19.69	−85.49	16.12
0600 UTC 11 Jul	—	—	20.40	−86.30	—

assumed to be horizontally homogeneous, then the horizontal derivative of this equation,

$$\Delta H = [(R/g)\Delta \overline{T}] \ln\left(\frac{p_1}{p_2}\right), \qquad (1)$$

gives the horizontal change in thickness (ΔH) for a given horizontal change in layer-mean temperature ($\Delta \overline{T}$). This assumption allows the horizontal change in temperature at a single level to be substituted for $\Delta \overline{T}$. In addition, the "D-value depression" is defined here as the decrease in D value (and thus the height of a pressure surface) from two points at 15 min of flight time at either side of the center to that at the center. When a flight path contains only a single radial leg, a one-sided difference is used. Equation (1) is applied in the following manner. Suppose the D-value depression at 850 hPa is 60 m, and the temperature at 850 hPa is 5°C warmer in the core than it is at the 100-km radius. Then the difference in the 850–700-hPa thickness between the center and 100 km is 28 m based on Eq. (1). That indicates that the 700-hPa D-value depression would be about half as large as at 850 hPa. The assumption of a horizontally uniform lapse rate used to derive Eq. (1) will never hold exactly. It will be shown in section 4b, however, that in the one instance in Hurricane Claudette where it could be tested, the estimated D-value depression at 700 hPa was within 15 m of the observed value.

b. *Storm track*

Table 1 shows that the linearly interpolated 6-hourly best-track positions from the National Hurricane Center (NHC) differ from real-time reconnaissance fixes by up to 39 km. These differences arise for two reasons: the storm location does not vary linearly over 6 h and the best track itself often requires some smoothing of high-frequency oscillations. Because reconnaissance data form the basis of this study, the real-time fixes in Table 1 are used to define the center. These positions are linearly interpolated in time to 1-min intervals (hereafter referred to as the interpolated reconnaissance track) in order to composite the data with respect to the moving center.

Radial velocity estimates are sensitive to errors in center position. To evaluate the uncertainty in such estimates, the center position is shifted by 10 km to the north, south, east, and west. The root-mean-square (rms) difference in radial velocity from these center shifts is indicated on the radial velocity plots (see Fig. 12). The values are accepted as meaningful only when the rms difference is much smaller than the calculated radial velocity.

Along-track relative vorticity is computed following Kossin and Eastin (2001, their section 2c). Each radial pass through the storm center is split into inbound and outbound legs, and the 10-s observations are interpolated to a 0.5-km radial grid. Relative vorticity is calculated using the storm-relative tangential wind, then smoothed using a 7-point Bartlett filter to remove oscillations with wavelengths less than ~4 km.

c. *Vertical wind shear*

Multiple estimates of 850–200-hPa vertical wind shear will be made by varying three quantities (see Table 2): the gridded analysis [the National Centers for Environmental Prediction (NCEP) versus the European Centre for Medium-Range Weather Forecasts (ECMWF)]; the center position (model-based using the 850-hPa vorticity maximum versus the NHC best track); and the radial range (0–500 and 200–800 km). All but the 200–800-km estimate are calculated following Corbosiero and Molinari (2002). The remaining value follows that of the Statistical Hurricane Intensity Prediction Scheme (SHIPS) database (see DeMaria et al. 2005).

Eastin et al. (2006) estimated shear from dual-Doppler winds based on 10 passes through the core of Hurricane Guillermo (1997). The mean Doppler esti-

TABLE 2. Parameters for each estimate of the vertical wind shear. Analyses are ECMWF Global Operational analysis, NCEP Final Global Data Assimilation System (FNL) analysis, and NCEP Global Forecast System (GFS) analysis.

Shear estimate identifier	Analysis	Center location	Area
ECMWF-BT	ECMWF (1.125° × 1.125°)	NHC best track	0–500-km disk
NCEP-BT	NCEP FNL (1° × 1°)	NHC best track	0–500-km disk
NCEP-VORT	NCEP FNL (1° × 1°)	Analysis 850-hPa vorticity max	0–500-km disk
SHIPS-BT	NCEP GFS	NHC best track	200–800-km annulus
SHIPS-OP	NCEP GFS	NHC operational track	200–800-km annulus

mate fell within 1 m s^{-1} in magnitude, and was almost identical in direction, to the SHIPS estimate. Braun et al. (2006) compared vertical shear within a high-resolution mesoscale model simulation of Hurricane Bonnie (1998) to estimates from the NCEP and ECMWF global analyses. The differences ranged from 0 to 3 m s^{-1}, and time variation was similar. These examples are limited in scope, but they suggest that the large-scale estimates contain useful information. The differences between the various estimates in this study will provide a measure of the uncertainty (see the following section).

3. Storm history and environment

Lawrence et al. (2005) give a full account of the history of Claudette. A brief summary of the evolution of Claudette and the environment in which the storm existed will be given here.

The easterly wave that became Claudette left the west coast of Africa on 1 July 2003. The wave tracked westward across the Atlantic Ocean for several days, strengthening slightly, but without developing a closed surface circulation. As Claudette passed over the island of St. Lucia at 2100 UTC 8 July, an advisory by the NHC declared the system a tropical storm retroactively to 1800 UTC. The storm continued westward at speeds of 10–12 m s^{-1} as it headed into the Caribbean Sea. Figure 1 shows the minimum central pressure and maximum surface wind speed from the NHC best track for the period 0000 UTC 7 July–0000 UTC 12 July.

By 0600 UTC 10 July, the storm's forward motion had slowed from 10 to 12 m s^{-1} toward the west to near 8 m s^{-1} toward the northwest. A USAF reconnaissance aircraft, which left the storm center at ~0745 UTC, reported winds of tropical storm strength. At this time the storm was also experiencing an increase in vertical wind shear, directed from the southwest. At 1200 UTC 10 July, a reconnaissance plane reported 850-hPa flight-level winds in excess of hurricane strength and a near-simultaneous dropsonde report showed surface winds also just over hurricane strength. A closed eyewall existed at the 20-km radius. This information warranted the upgrade of Claudette to a category 1 hurricane in the postseason analysis. Figure 1 shows a sharp pressure fall of 10 hPa and an increase in the maximum sustained winds from 28 to 36 m s^{-1} between 0600 and 1200 UTC 10 July.

The hurricane-strength circulation lasted less than 6 h; a penetration through the storm at ~1700 UTC failed to find a clear circulation center at the 700-hPa flight level. The storm's appearance in satellite imagery deteriorated over the next few hours as the cloud tops over the storm center warmed and the focus of the deep convection shifted toward the northeast, away from the storm center. The NHC best track shows the maximum sustained winds fell to 28 m s^{-1} by 1800 UTC, further dropping to 25 m s^{-1} by 0000 UTC 11 July (Fig. 1). During the 6-h period from 1200 to 1800 UTC, the storm filled at a rate of 2.5 hPa h^{-1}, and the central pressure continued to rise over the subsequent 6 h. Claudette did not become a hurricane again for 4 days.

Figure 2 shows the track of Claudette through the western Caribbean Sea from 0000 UTC 10 July to 0000 UTC 11 July 2003, the same 24-h period indicated by the shading in Fig. 1. Also shown are 3-day composite sea surface temperatures (SSTs), for the period 7–9 July, from the Advanced Microwave Scanning Radiometer (AMSR-E) aboard the National Aeronautics and Space Administration (NASA) *Aqua* satellite (Chelton

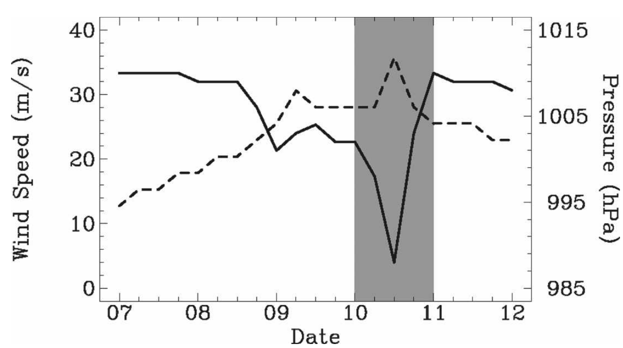

FIG. 1. Minimum central pressure (hPa, solid line) and maximum sustained surface wind speed (m s^{-1}, dashed line) at 6-h intervals from 0000 UTC 7 Jul to 0000 UTC 12 Jul 2003, from the NHC best track. The shaded area identifies the case study period.

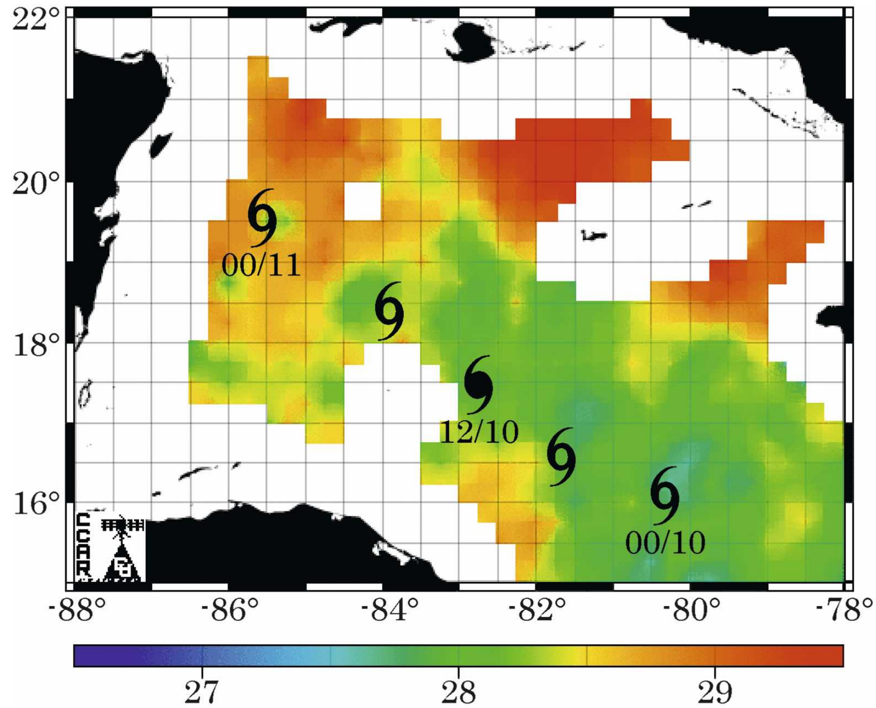

FIG. 2. Mean 3-day SST (°C, shading) for the period 7–9 Jul 2003 in the western Caribbean Sea, and interpolated reconnaissance track (see section 2 for further details) at 6-h intervals (symbols; open for tropical storm, filled for hurricane). The SST plot is courtesy of the Colorado Center for Astrodynamics Research at the University of Colorado (see online at http://argo.colorado.edu/~realtime/global-sst/).

and Wentz 2005). The data are not available within 75 km of land. A 3-day composite is chosen to allow sufficient coverage by the polar-orbiting satellite. The 3 days prior to the passage of the storm are chosen to avoid incorporating any SST changes due to the tropical cyclone itself.

As Claudette moved northwestward over the 24-h period shown, the storm passed over gradually increasing SSTs, with the highest temperature water (29.0°C) encountered at ~2100 UTC 10 July. During the intensification phase (0600–1200 UTC), the SSTs under Claudette remained approximately constant at ~28.2°C, but increased slightly to 28.4°C during the following 6 h, while Claudette rapidly weakened. Because of the small change in SSTs along the track of Claudette, it is surmised that the intensity changes of the storm were not the result of forcing by the ocean below the storm. Similar 3-day composites of SST from after the passage of Claudette show similar values along the track of the system, suggesting that the rapid decay was not caused by storm-induced cooling.

A weak upper-tropospheric trough existed ~600 km northwest of Claudette at 0000 UTC 10 July. The trough moved westward at about the same speed as the storm. As a result, it did not produce sufficient flux convergence of angular momentum to meet the definition of a trough interaction by Hanley et al. (2001). It is concluded that a favorable trough interaction did not cause the intensification of Claudette.

Figure 3 shows the magnitude and direction of the 850–200-hPa vertical wind shear at each of the 6-h times shown in Fig. 2. Five different estimates of the shear are shown (see Table 2 for definitions). The direction of the shear (Fig. 3a) was consistently from the southwest for all time periods and for all the estimates. The difference in shear magnitude by the various estimates (Fig. 3b) was as large as 8 m s^{-1}. If the mean shear magnitude line in Fig. 3b were taken at face value, changes in shear would be exactly of the wrong sign to account for the intensity change. The uncertainty is large enough, however, that the small calculated changes in shear magnitude during the period of interest are not meaningful. Two conclusions appear justified: vertical wind shear remained large throughout the period, and changes in shear did not cause the dramatic deepening and filling of Claudette.

Figure 4 shows Quick Scatterometer (QuikSCAT) surface wind vectors (Lungu 2001; Hoffman and Leidner 2005) and the interpolated reconnaissance storm center location at 1057 UTC 10 July. The wind

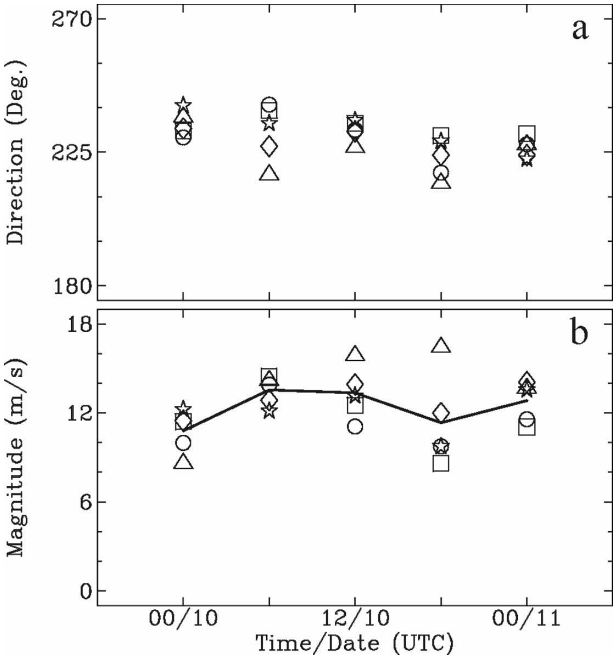

FIG. 3. Estimates of 850–200-hPa vertical wind shear: (a) direction (°) and (b) magnitude (m s^{-1}), every 6 h from 0000 UTC 10 Jul to 0000 UTC 11 Jul 2003. The different estimates of shear are identified as follows (see Table 2 for definitions): ECMWF-BT (triangle), NCEP-BT (circle), NCEP-VORT (square), SHIPS-BT (diamond), and SHIPS-OP (star). The solid line in (b) represents the mean of the five estimates of shear magnitude. See text for further details.

field depicts the structure of the large-scale easterly wave in which Claudette was embedded. The strongest winds were located within 50 km of the center, to the northeast. Winds in excess of 35 kt (18 m s^{-1}) were present over a large area north and northeast of the storm center. This strong wind area correlates well with the location of the majority of the deep convective cells that composed the system (see Fig. 5, discussed below).

4. Development and decay of the hurricane structure

a. Convective structure

Figure 5 shows the evolution of the convection within Claudette at 6-hourly intervals from 0000 UTC 10 July to 0000 UTC 11 July. Each panel of this figure depicts an IR satellite image (at 15 min after the standard analysis time), the storm center location at the analysis time, and up to 4 h of reconnaissance wind observations centered on the analysis time. The latitude and longitude lines (and geography) are provided for reference to the IR imagery only; the wind observations are composited about the moving storm center and therefore do not relate to the geography. All center locations represent those from the interpolated reconnaissance track described in section 2.

At 0000 UTC 10 July (Fig. 5a), the storm center was located close to the outer edge of the cirrus shield. The deepest convection existed approximately 100 km downshear (northeast) of the center. The reconnaissance observations from the 850-hPa flight level reveal a closed circulation embedded within a larger-scale wavelike flow. The strongest winds were found on the northeast side of the storm under the deep convection, consistent with the west-northwesterly storm motion. Removal of the storm motion from the wind observations reveals a near-symmetric circulation (not shown). Over the next 6 h convection developed closer to the center and by 0600 UTC 10 July (Fig. 5b), the deepest convection (identified by cloud tops colder than −80°C) was located approximately 50 km north-northeast (downshear left) of the center. The storm center was located near the center of the cirrus outflow from this strong cell. The reconnaissance observations (again at the 850-hPa flight level) show a similar structure to the previous time, but with stronger winds on the northeast and southeast flight legs, and weaker winds on the southwest leg. By 1200 UTC 10 July (Fig. 5c), the deep convection had become well established over the center. The 700-hPa flight-level observations show a well-established central circulation. Inset into the lower left of Fig. 5c are observations from the 850-hPa flight level near 1200 UTC 10 July. During the approach to the storm center on the south-southwest side of the storm, the radius of maximum wind (RMW; ~10 km) can be identified by the 30 m s^{-1} wind barb. On the north side of the storm, the RMW cannot be determined due to an abrupt change of flight level, but the aircraft did encounter winds in excess of 40 m s^{-1} at ~8-km radius prior to ascending. As noted earlier, Claudette was at hurricane strength at this time, as evidenced by the surface wind (shown in red) from the 1203 UTC dropsonde in the Fig. 5c inset.

The cloud tops over the center warmed over the next 6 h (Fig. 5d), and the deep convection returned to downshear. In a flight just prior to 1800 UTC, USAF reconnaissance found no significant *D*-value minimum at 700 hPa (see Fig. 11). Claudette was downgraded to a tropical storm at 1800 UTC. The weakening trend continued over the next few hours as downshear convection increased in intensity. By 0000 UTC 11 July (Fig. 5e) convection was present only on the downshear half of the storm, and reconnaissance observations at the 850-hPa flight level show wind speeds generally less than 20 m s^{-1} and little evidence of a circulation center.

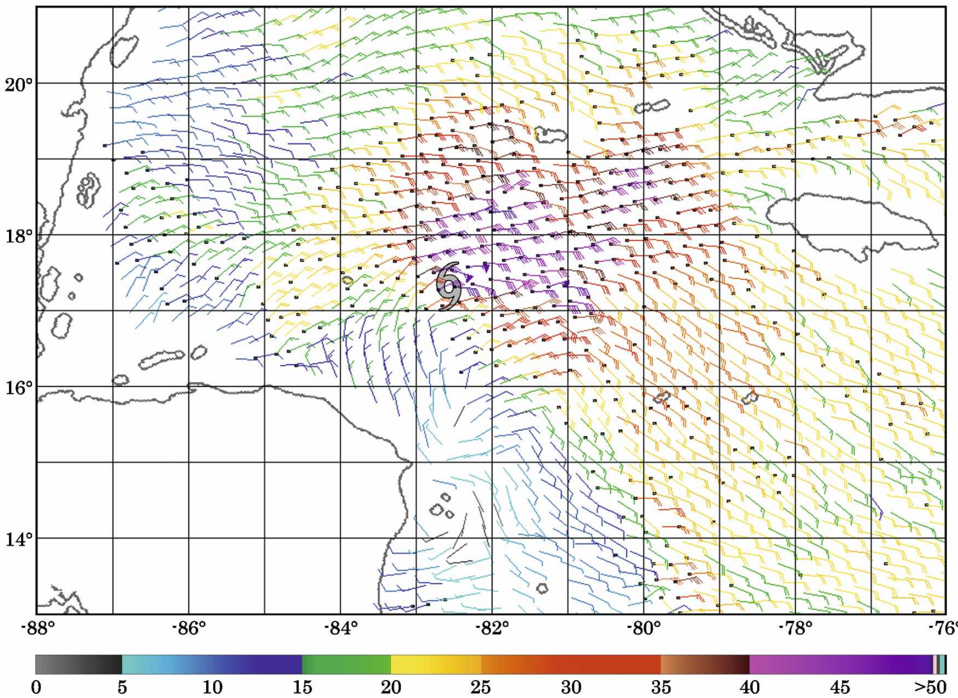

FIG. 4. QuikSCAT ocean surface wind vectors (kt) at 10-m altitude and the interpolated reconnaissance center location (gray tropical storm symbol) at 1057 UTC 10 Jul 2003. Vectors are plotted at 25-km resolution. Image courtesy of the Marine Observing Systems Team at the NOAA/National Environmental Satellite, Data, and Information Service (see online at http://manati.orbit.nesdis.noaa.gov/cgi-bin/qscat_storm.pl).

A somewhat similar series of events occurred the previous day, early on 9 July 2003. Lawrence et al. (2005) commented that Claudette may have reached hurricane intensity briefly, but the near-surface wind strength could not be verified without a dropsonde. This event could not be investigated further.

The intensity changes Claudette underwent are exemplified by the evolution of the convection. Whether cause or effect, the proximity of deep convection to the vortex center correlated well with the intensity of Claudette, a phenomenon previously described by Dvorak (1984).

b. Flight-level observations

Flight-level observations are used to show the evolution of the thermodynamic and kinematic structure of Claudette as the system rapidly strengthened and weakened. Figures 6–9 show time series of various thermodynamic and kinematic variables collected by USAF reconnaissance. Each time series spans 30 min, which equates to a distance of about 180 km, centered on the time the aircraft passed through (or closest to) the storm center. The direction of the observations from the storm center is given for reference at the start and end points of the flight pass at the base of each figure. In some cases, the time axis [along the base of panel (d) in each figure] is reversed for ease of viewing, so the westernmost observations are always on the left side and easternmost on the right. In the following time series, *storm-relative* tangential wind speed will be shown, and equivalent potential temperature (θ_e) is calculated following Bolton (1980).

The USAF flew through the center of Claudette (from downshear to upshear) near 0600 UTC 10 July, prior to the rapid intensification. Figure 6 shows the time series for this flight at the 850-hPa flight level. The tangential wind observations show a fairly symmetric (storm relative) circulation existed at this time (Fig. 6d), with wind speeds of the order 10–15 m s^{-1}. The wind speed minimum at the vortex center was accompanied by a weak pressure minimum (Fig. 6c). The vortex center was characterized by a warm core with a temperature maximum near 25°C and dewpoint depressions near 8°–10°C (Fig. 6b). Outside the core, temperatures were about 17°–19°C and the air was relatively moist. These temperature and dewpoint structures give rise to the θ_e profile shown in Fig. 6a. The maximum in θ_e existed near the vortex center, typical of a tropical storm at this flight level (Shelton 2005).

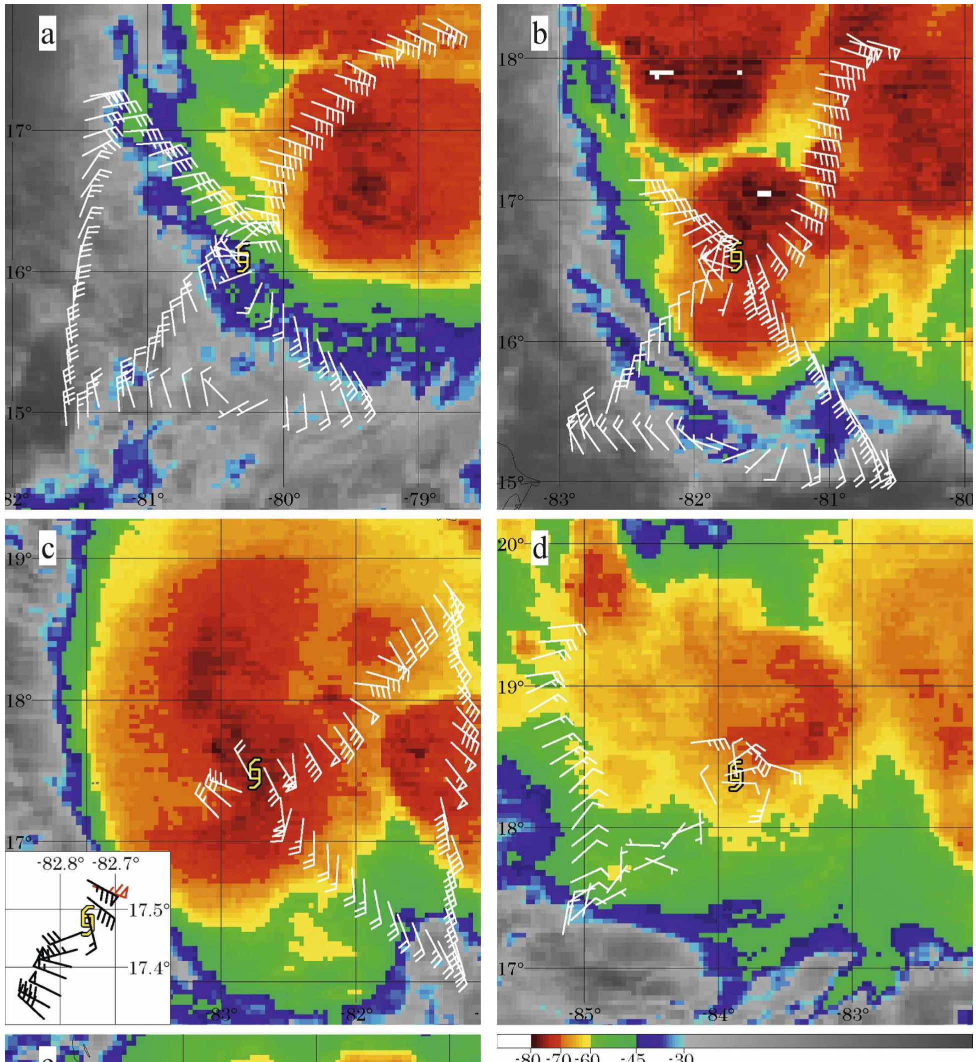

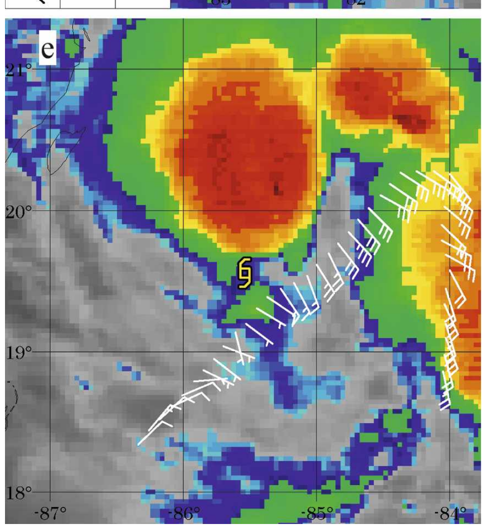

FIG. 5. Color-enhanced IR satellite imagery (brightness temperatures in °C) centered on the interpolated reconnaissance track storm center (yellow and black tropical storm symbol), overlain with up to 4 h of reconnaissance wind observations composited about the moving storm center, for (a) 0000 UTC (winds at 850 hPa), (b) 0600 UTC (winds at 850 hPa), (c) 1200 UTC (winds at 700 hPa), (d) 1800 UTC 10 Jul (winds at 700 hPa), and (e) 0000 UTC 11 Jul 2003 (winds at 850 hPa). IR images are from 15 min after the analysis time. Winds are plotted every 2 min, except within 50 km of the center in (d) where the winds are plotted every 6 min. Wind observations are plotted as follows: half barb = 2.5 m s^{-1}, full barb = 5 m s^{-1}, and pennant = 25 m s^{-1}. Image scale approximately 400 km × 400 km. Inset in (c) shows 5 min of reconnaissance wind observations at the 850-hPa flight level, plotted every 30 s (black), and the surface wind observation from the 1203 UTC dropsonde (red). Inset scale is approximately 30 km × 30 km.

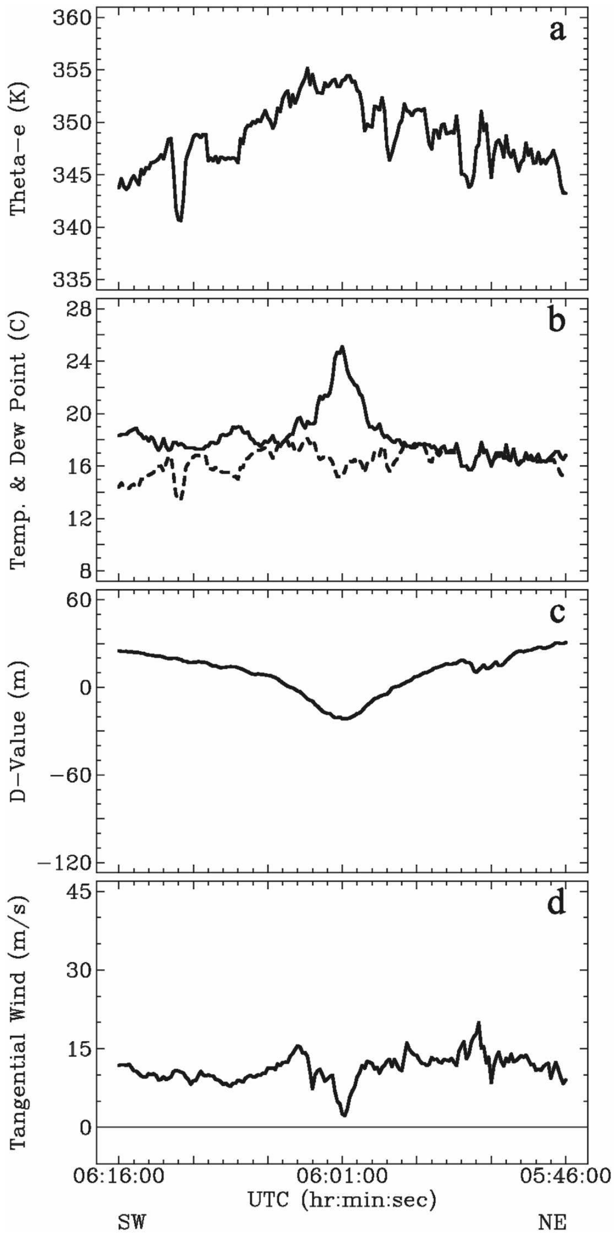

FIG. 6. Time series of observations for a 30-min period, at the 850-hPa flight-level, beginning at 0546 UTC 10 Jul 2003 and ending at 0616 UTC as the USAF aircraft passed through Claudette from northeast to southwest: (a) θ_e (K), (b) temperature (solid, °C) and dewpoint (dashed, °C), (c) D value (m), and (d) storm-relative tangential wind speed (m s^{-1}).

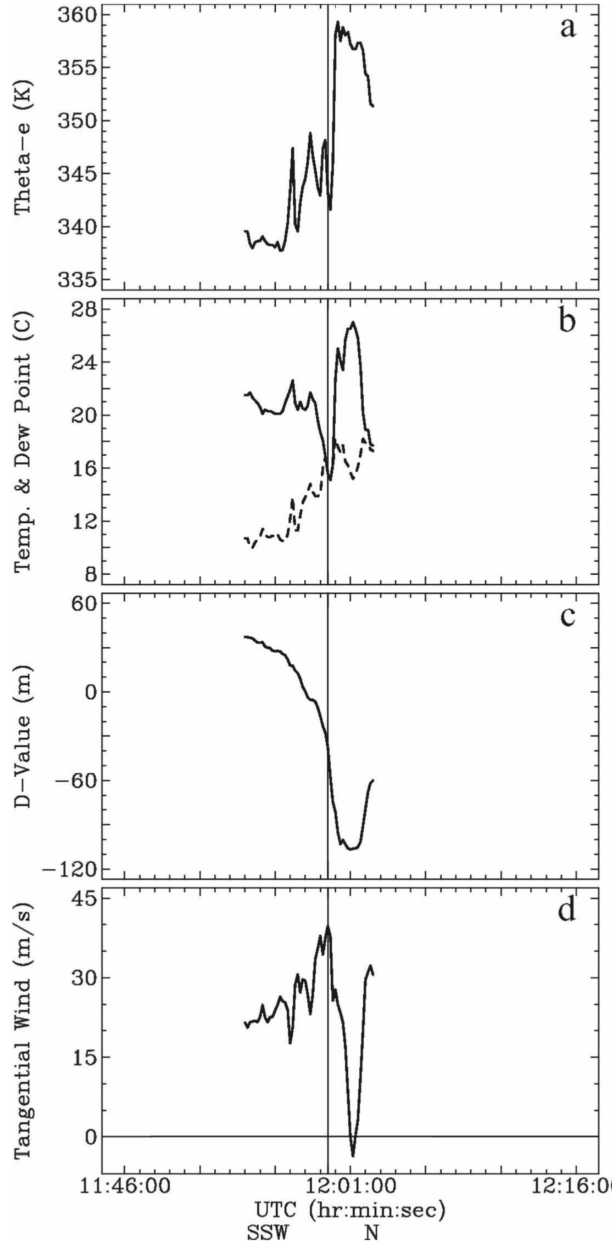

FIG. 7. As in Fig. 6, but for observations from 1154:00 UTC 10 Jul to 1202:30 UTC 10 Jul 2003. Aircraft passed from south-southwest to north. Vertical line identifies the radius of maximum winds (see text for further details).

From Fig. 6b, the $\Delta\overline{T}$ between the core and its immediate environment was 7.6 K. Using Eq. (1), the excess in 850–700-hPa thickness between the storm center and the edge of the pass was 43.1 m. The D-value depression at 850 hPa was 49.5 m (Fig. 6c). Applying the thickness change, the estimated D-value depression at 700 hPa was 6.4 m. To the extent that Eq. (1) is valid, this indicates the vortex was only about 3 km deep at 0600 UTC 10 July.

Figure 7 shows time series at 850 hPa for a pass through the center of Claudette 6 h after that shown in Fig. 6. In the postseason analysis (Lawrence et al. 2005), Claudette was named a hurricane based on near-surface wind observations (from a dropsonde) during this pass. The observations shown in Fig. 7 begin approximately 36 km south-southwest of the center and end about 8 km to the north. Thereafter the aircraft climbed to 700 hPa.

In all the time series in Fig. 7, the structure of the storm has changed remarkably since the previous flight (Fig. 6). Maximum storm-relative tangential wind speeds (Fig. 7d) increased to 40 m s^{-1}, consistent with the increased pressure gradient (Fig. 7c). The USAF flew through the RMW on the south-southwest side of the storm at approximately 1159:30 UTC, about 10 km from the center. Collocated with this tangential wind maximum was a cool, saturated region in the temperature and dewpoint time series (Fig. 7b), which is indicative of an eyewall. Evidence for the beginnings of a wind speed maximum and eyewall on the north side were observed just prior to the aircraft climbing to a higher level. In the eye, the air was ~2°C warmer than 6 h before. Dewpoint temperatures were comparable, resulting in a higher θ_e maximum (~358 K, Fig. 7a) at the center. The dewpoint depression in the eye increased to 10°–12°C. One important feature in Fig. 7b that will be discussed shortly is the dry air south-southwest of the storm center.

Approximately 2 h later, the USAF again passed through the center of Hurricane Claudette, but at a flight level of 700 hPa. Figure 8 shows a transect from northeast to southwest (downshear to upshear). The RMW on both sides of the storm center is distinguishable in the storm-relative tangential wind speed time series (Fig. 8d). On the upshear side, the USAF encountered the RMW at about 1354:10 UTC (~13-km radius), while downshear the RMW was found at 1348:30 UTC (~25-km radius). The weaker maximum tangential wind speeds and smaller horizontal D-value gradient (Fig. 8c) observed on this pass at 700 hPa compared with those observed during the previous pass at 850 hPa are consistent with a warm-core vortex in which the strength of the vortex decreases with altitude. Again, Eq. (1) can be used to infer details of the vertical structure of Claudette. From Figs. 7b,c, $\Delta\overline{T}$ was 4.9 K and the D-value depression was 143.8 m at 850 hPa at ~1200 UTC 10 July. Using Eq. (1), the D-value depression at 700 hPa would have been 116.1 m at this time. From Fig. 8c, at ~1400 UTC, the observed D-value depression at 700 hPa was 101.8 m. The similarity of the calculated and observed D-value depressions supports the use of Eq. (1). If Eq. (1) is applied again using the 700-hPa temperature field near 1400 UTC, the calculated D-value depression at 500 hPa would have been 51 m. Thus, a storm that barely reached 700 hPa at 0600 UTC appeared to extend beyond 500 hPa at 1400 UTC. The storm had both strengthened and deepened in the 6 h between reconnaissance flights and had continued to do so through 1400 UTC.

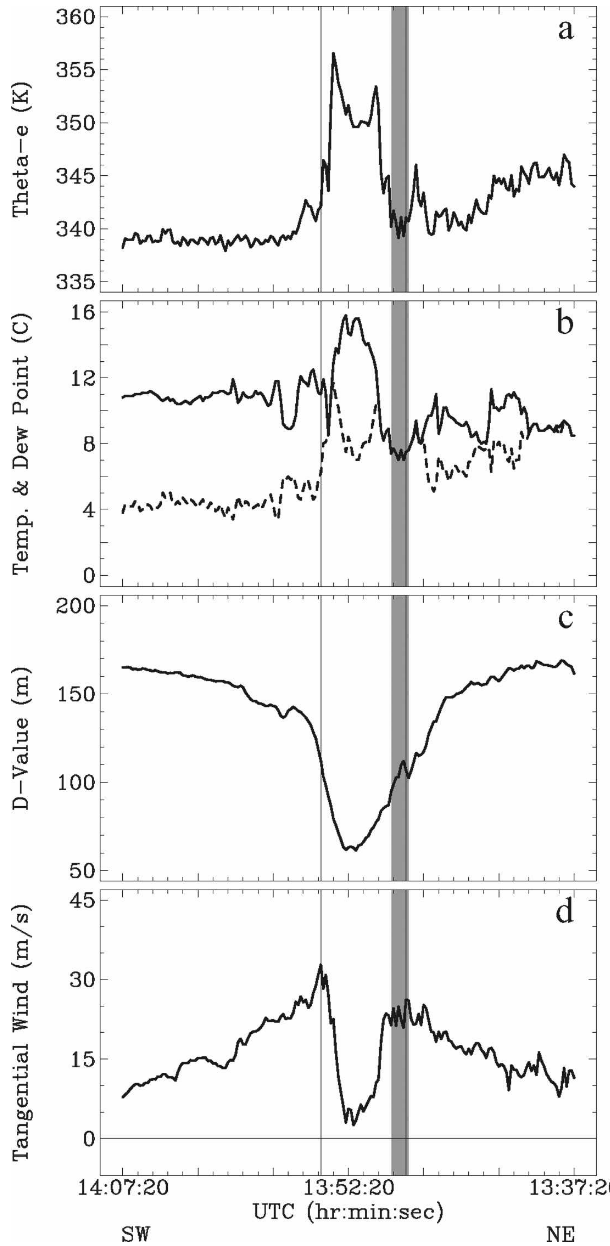

FIG. 8. As in Fig. 7, but for observations at the 700-hPa flight level from 1337:20 UTC 10 Jul to 1407:20 UTC 10 Jul 2003. Shading identifies suspected instrument-wetting events (see text for further details).

Both the kinematic and thermodynamic fields from the center pass near 1400 UTC show structures consistent with a well-formed hurricane vortex. For example, the temperature and dewpoint profiles in Fig. 8b show saturated eyewall features (just radially inward from the RMW) that surround the warm (16°C) and dry (dewpoint depressions near 8°C) eye at the storm center. The highest θ_e was located in the saturated eyewall with lower, but still elevated, θ_e values inside the eye.

This θ_e structure is consistent with the observations of Kossin and Eastin (2001) for intensifying hurricanes. One field, however, differs dramatically: the moisture field. Dry air, with dewpoint depressions as large as 10°C, existed immediately adjacent to the eyewall on the upshear side at both 850 (Fig. 7b) and 700 hPa (Fig. 8b). This dry air extended at least to the 100-km radius. Unusually low θ_e values and a strong radial gradient of θ_e (exceeding 6 K km^{-1}) existed upshear near the core. Strong radial gradients of θ_e are known to occur near the hurricane eyewall, as shown by Hawkins and Imbembo (1976). These gradients were, however, not accompanied by low relative humidity air outside the eyewall. Rather, Hawkins and Imbembo (their Fig. 12) show relative humidity above 90% throughout and beyond the region of strong θ_e gradient. The extremely dry air shown in Hurricane Claudette so close to the eyewall in the lower troposphere is rare in a hurricane-strength disturbance. M. D. Eastin (2008, personal communication; see also Eastin et al. 2005) described only two comparable examples at or below 850 hPa in a multiyear dataset. In contrast to the upshear side of Hurricane Claudette, the air downshear was relatively cool and moist (dewpoint depressions generally <4°C).

The reconnaissance aircraft passed through the center of Claudette once again near 1530 UTC (Fig. 9), from southeast to northwest (right-of-shear to left-of-shear). The maximum storm-relative tangential wind speed, located on the southeast side of the storm (1525:40 UTC; ~8-km radius), was higher than in the previous, perpendicular, pass through Claudette. A dropsonde released at 1526 UTC observed 47 m s^{-1} winds at 976 hPa, with a mean boundary layer wind estimated at 41 m s^{-1}, confirming Claudette was still a hurricane at ~1530 UTC. Other changes, however, suggest a storm in transition. The eye temperature had cooled to 14°C (Fig. 9b) and the dewpoint had risen, resulting in a slightly moister eye. The pressure gradient fell to almost zero on the left-of-shear side of the storm after ~1528 UTC flight time (i.e., beyond the 15-km radius; Fig. 9c). Consistent with this, the tangential winds there were weak and highly variable. Unfortunately, a suspected sensor wetting error (shaded) just northwest of the storm center complicates interpretation, but the remaining fields suggest that the eyewall structure on the left-of-shear side had been disrupted. The presence of dry air on both the left- and right-of-shear sides of the storm resulted in low θ_e values everywhere except at the very center of the vortex. The presence of a single maximum in θ_e is consistent with that observed by Kossin and Eastin (2001) in weakening systems. Overall, although Claudette was still a hurricane at 1530 UTC, there was evidence of eyewall disruption and much lower wind speeds on the northwest (left of shear) side of the storm.

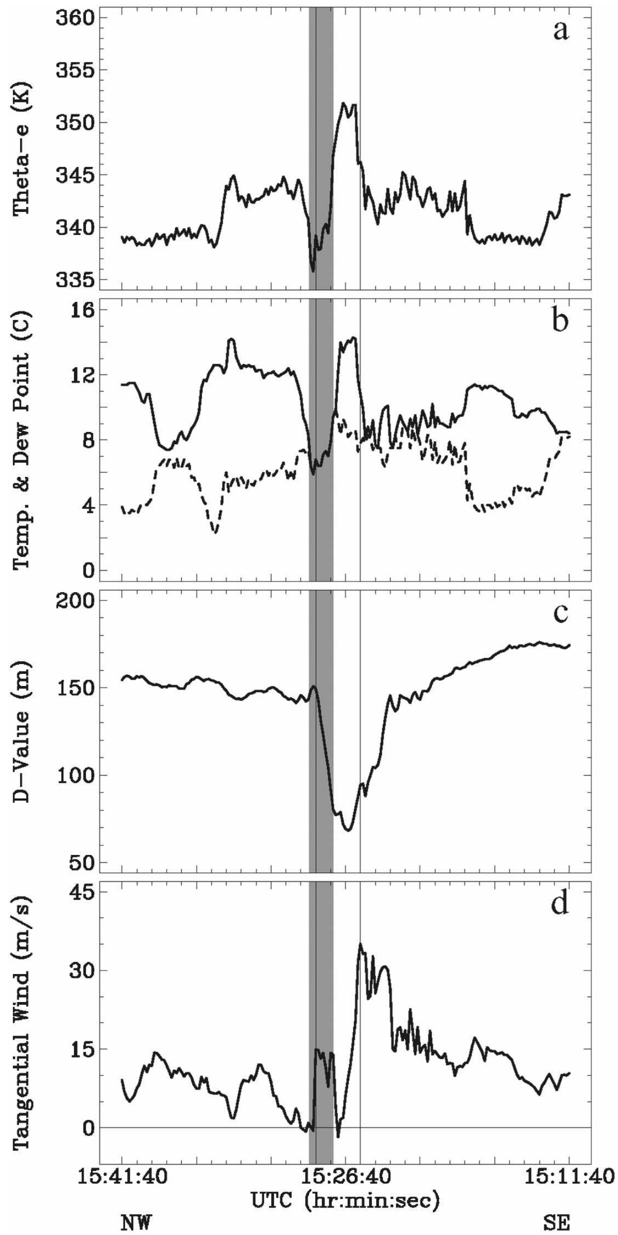

FIG. 9. As in Fig. 8, but for observations from 1511:40 UTC 10 Jul to 1541:40 UTC 10 Jul 2003. Aircraft passed from southeast to northwest.

Figure 9b shows evidence for precipitation-induced cooling in the dry air upshear of the center (flight times 1536–1539 UTC, approximately 60–85-km radii). In particular, temperature dropped and dewpoint rose to produce near saturation in the absence of any significant perturbation in θ_e (which would not be altered by evaporation of precipitation). This region is well outside the core, however, and comparable evidence in the

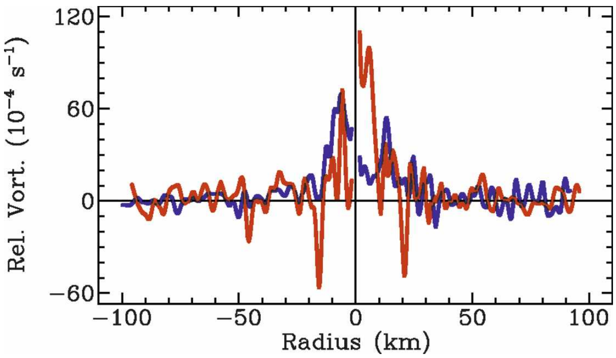

FIG. 10. Radial distribution of relative vorticity (10^{-4} s^{-1}) for the 1352 UTC (blue; northeast–southwest) and 1526 UTC 10 Jul 2003 (red; southeast–northwest) radial passes through the center of Claudette. The passes have the same orientation as their respective time series (either Figs. 8 or 9) such that the easternmost observations are on the right of the figure. See section 2b for details on the relative vorticity computation.

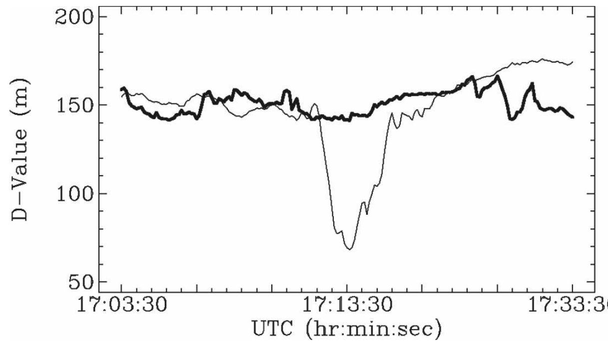

FIG. 11. Time series of the D value (m) at 700 hPa for 1703:30–1733:30 UTC 10 Jul 2003 (thick line). The D-value trace from Fig. 9c (thin line) is provided for reference.

vicinity of the eyewall is lacking. The wetting errors in the northwest eyewall make further interpretation difficult, but precipitation evaporation near the northwest eyewall where the wind speeds collapsed seems unlikely.

Because the flight tracks in Figs. 8 and 9 are perpendicular, the differences in structure could relate in part to azimuthal asymmetries. It is argued that the differences reflect changes in time in the structure of the storm, for the following reasons. 1) The winds northwest of the center in Fig. 9 are far below those at the other azimuths in Figs. 8 and 9. Such a structure is not representative of the azimuthal wavenumber 1 or wavenumber 2 structures that we might expect based on the work of Marks et al. (1992). 2) HRD H*Wind analyses (Powell et al. 1998) valid at 1330, 1630, 1930, and 2230 UTC 10 July (not shown) do exhibit azimuthal asymmetries. However, they also display enormous temporal variations in the surface wind field between 1630 and 2230 UTC. 3) The flight from 90 min after the time of Fig. 9 (discussed below) shows a remarkable change in the D-value structure. Taken together, this evidence suggests that the storm was experiencing rapid time changes, and these are likely to dominate any azimuthal variations between the two cross-section directions shown in Figs. 8 and 9.

Figure 10 shows radial profiles of relative vorticity (refer to section 2b for further details) for the two passes through the center of Claudette at 1352 and 1526 UTC. During the earlier flight, relative vorticity maxima were present either side of the storm center at 13 and −6 km (~10 km radially inward from each RMW) with values of 54.2 and 69.5 × 10^{-4} s^{-1}, respectively. Kossin and Eastin (2001) identified similar eyewall vorticity maxima as indicative of a strengthening hurricane (their "regime 1"). The later flight exhibited maximum relative vorticity of 110 × 10^{-4} s^{-1} just southeast of the storm center, within the eye. Kossin and Eastin (2001) observed similar center vorticity maxima in storms undergoing weakening (their "regime 2"). The significance of these structures will be addressed in the discussion.

Near 1700 UTC the USAF attempted to fly through the center of Claudette once again at 700 hPa. However, as the aircraft passed through the assumed location of the storm center from the southwest, a flight-level circulation could not be found. The USAF was unable to accurately fix the storm center location for the 1800 UTC NHC advisory. The time series of observations for this center pass are not shown here because of the complexity of the flight track. However, Fig. 11 shows a time series of D-value observations for a 30-min portion of this final pass through Claudette. The time interval chosen does not represent a period centered on the vortex as in the previous figures, but rather is selected to include the lowest D-value observations measured for this pass. The difference between the maximum and minimum D-value observations is less than 30 m, implying the deep low seen 2 h earlier (also shown in Fig. 11 for reference) had almost completely disappeared at this level. Consistent with this, flight-level winds observed at this time were weak tropical storm strength (generally less than 15 m s^{-1}), with maximum winds <23 m s^{-1}. The hurricane structure had been lost between 1530 and 1700 UTC, at least at the 700-hPa flight level.

An obvious question ensues: how and why did the 700-hPa circulation weaken so quickly? Some insight can be gained through consideration of the storm-relative radial flow at flight level. Figure 12 shows the radial wind component for the two passes through the center of Claudette shown in Figs. 8 and 9. The solid

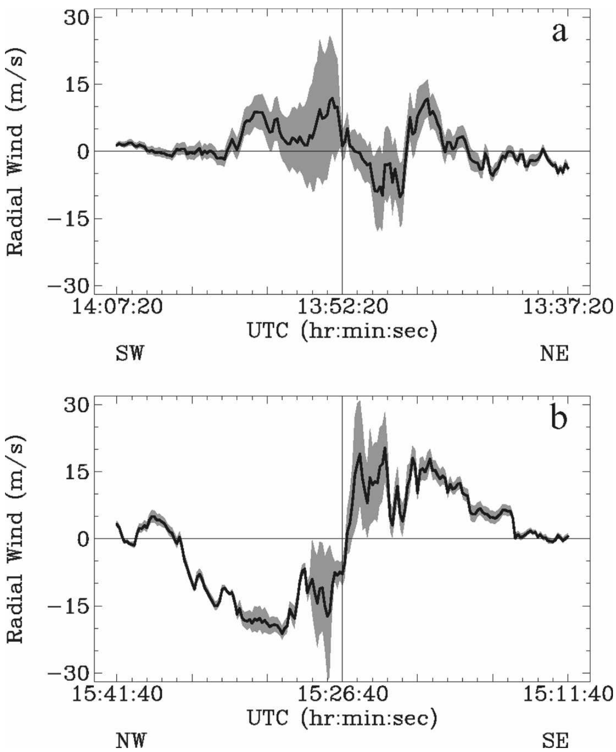

FIG. 12. Time series of storm-relative radial wind speed (solid line, m s^{-1}) at the 700-hPa flight level for (a) 1337:20–1407:20 UTC 10 Jul 2003 (northeast–southwest) and (b) 1511:40–1541:40 UTC 10 Jul 2003 (southeast–northwest). Shading indicates uncertainty in the calculated value based on a series of 10-km displacements in storm center location (see text for further details).

line is the radial wind calculated using the reconnaissance wind observations and the center location. The size of the shaded region provides a measure of uncertainty as described in section 2b. For the 700-hPa downshear-to-upshear pass through Claudette near 1400 UTC (Fig. 12a) the uncertainty is large near the center (i.e., between about 1348:20 and 1356:20 UTC). As a result, this region will not be discussed. Beyond this region near 1358:20 and 1346:20 UTC (i.e., at approximately 35–40-km radius), about 10 m s^{-1} outflow existed both upshear and downshear.

Figure 12b shows the radial wind during the right-of-shear to left-of-shear pass through the center of Claudette at ~1530 UTC. Immediately noticeable is the overall increase in the magnitude of the radial motion from the perpendicular pass 90 min previously. Strong (>15 m s^{-1}) inflow existed on the northwest side of the storm and strong outflow on the southeast side, indicating direct ventilation of the center at 700 hPa. The uncertainty associated with this cross-storm flow is generally small. The location of the inflow to the northwest of the center coincides with that of the dry air identified earlier in the temperature and dewpoint time series (Fig. 9b). The physical implications arising from the collocation of these thermodynamic and kinematic features are discussed in the following section.

5. Discussion

Tropical Storm Claudette deepened to hurricane strength during a 10-hPa fall in minimum central pressure over 6 h, then filled by 15 hPa in 6 h, and 22 hPa in 12 h (Fig. 1). Deep-layer vertical wind shear remained large during both intensification and filling. Sea surface temperature under the storm varied little throughout the period. No significant interaction with upper-tropospheric troughs occurred. None of these factors appeared to play any direct role in the rapid intensity changes. In this section the possible mechanisms for deepening and filling will be discussed.

a. *Intensification*

At 0000 UTC 10 July the strongest convection existed nearly 100 km downshear from the center of Claudette (Fig. 5a). Over the following 12 h, despite the presence of substantial vertical wind shear, convection moved inward toward the center. A Tropical Rainfall Measuring Mission (TRMM) Precipitation Radar overpass from 0645 UTC (not shown) showed at least one pixel of "storm height" (a derived quantity in the 2A23 product) above 15 km close to the storm center. Kelley et al. (2004) found such tall towers to accompany deepening 70% of the time. Consistent with their results, Claudette became a hurricane within 6 h.

With one reconnaissance flight near 0600 UTC and a second flight not until 1200 UTC, it was difficult to diagnose the reasons for the inward shift of convection. QuikSCAT (Fig. 4) at 1057 UTC showed strong winds (with respect to the surface) in a wide region north of the center, but light winds south of the center. The convection thus developed in the region where surface fluxes were likely strongest. The convective outbreak throughout the 12 h prior to hurricane intensity appeared in satellite animations to occur in the form of intense individual cells. This finding suggests a role for "vortical hot towers" (Hendricks et al. 2004; Montgomery et al. 2006), in which intensification occurs not as a result of uniform inflow and upward motion in the storm core, but rather as an upscale transfer of energy and angular momentum from a group of individual cells.

The U.S. Air Force Reserve reconnaissance aircraft data at the 850-hPa level near 0600 UTC showed clear evidence of an eye, with a 5°C warm anomaly and a

10°C dewpoint depression at the center (Fig. 6b). However, the storm-relative tangential wind profile was flat with values of only 10–15 $\mathrm{m\,s^{-1}}$ (Fig. 6d) and the θ_e maximum was broad (Fig. 6a). Evidence was presented that the vortex did not extend above 700 hPa.

Over the following 6 h as convection continued to move toward and eventually into the center of the storm, rapid development ensued. At hurricane intensity near 1200 UTC 10 July, the 850-hPa structure had dramatically changed from 6 h earlier. Maximum winds reached hurricane force only 10 km from the center (Fig. 7d). The eye had warmed about 2°C (Fig. 7b) producing a sharp θ_e maximum in the core (Fig. 7a), with clear evidence of an eyewall. Unexpectedly, the dewpoint temperatures upshear of the center fell substantially during the 6-h period of intensification. A coincident rise in temperature of ~2°–3°C in the same region produced dewpoint depressions close to 10°C within 100 km of the center, and 7°C immediately outside the upshear eyewall. Such warming and increase in dewpoint depressions is indicative of subsidence.

The 850-hPa flight level had to be abandoned as the system strengthened, but the reconnaissance aircraft crossed the center 2 h later (near 1400 UTC 10 August) at 700 hPa. The structure at that time resembled an intensifying hurricane (Kossin and Eastin 2001), with an eye and eyewall, dual θ_e maxima just inside sharp wind maxima, and strong radial θ_e gradients just outside the eyewall (Fig. 8). The RMW at 700 hPa occurred at the 13- and 25-km radii upshear and downshear, respectively. Once again, however, the lowest θ_e and extremely dry air existed upshear of the eyewall.

As noted in section 4b, although strong radial gradients of θ_e are known to occur near the eyewall (Hawkins and Imbembo 1976), relative humidity below 60% in the lower troposphere immediately adjacent to the eyewall is rare. It is hypothesized that the dry air in Claudette in the presence of continuing large vertical wind shear played a major role in the filling of the storm, as discussed in the following section.

b. Weakening

Reconnaissance aircraft revisited the storm at 700 hPa near 1530 UTC, only about 90 min after the previous flight. This flight was from right to left with respect to the vertical wind shear vector. The storm structure had substantially changed. Although hurricane-force winds existed right of shear (Fig. 9d), the left-of-shear side showed only 15 $\mathrm{m\,s^{-1}}$ tangential winds. Strong inflow was present within and radially outside of this region. The eye had cooled by 2°C (Fig. 9b). Dry air existed adjacent to the eyewall left of shear, the same region where the wind speed had fallen and where significant inflow was present. The storm rapidly weakened thereafter. Only a small D-value depression existed at 700 hPa 2 h later at 1730 UTC, and reconnaissance aircraft could not find a closed circulation even at 850 hPa by 0000 UTC the following day.

Any process that produces cooling of the tropical cyclone core will create pressure rises that reduce the radial pressure gradient and thus the maximum winds. If cooling reaches the surface, subsequent convection is suppressed as well. The presence of dry air adjacent to the eyewall in a storm experiencing vertical wind shear could produce weakening by a number of processes: cooling due to precipitation falling from above into dry air; ventilation of the storm (Simpson and Riehl 1958; Cram et al. 2007) as vertical wind shear carries the dry, lower θ_e air into the core; and dry air intrusion as a result of eyewall breakdown and subsequent lateral mixing (Kossin and Eastin 2001). These processes will be addressed in sequence.

Cold, precipitation-forced downdrafts (e.g., those that form within hurricane rainbands) that reach the surface can modify the boundary layer inflow air. If the boundary layer θ_e is reduced sufficiently by these downdrafts, it will not have enough time to recover (through mixing and increases due to surface fluxes) to premodification values prior to being ingested into the eyewall (Powell 1990). As noted earlier, evidence existed for precipitation-induced cooling northwest of the center at approximately 60–85-km radii. Cold downdrafts related to this may well have been present, but it is unlikely that modified boundary layer could have reached the eyewall and undermined the convection on the short time scale that Claudette evolved. Within the eyewall, instrument-wetting errors made interpretation of the thermodynamic fields difficult. The role of rainfall evaporation in the weakening of Claudette remains uncertain.

Ventilation would be likely to occur as a result of vertical wind shear, as shown by Cram et al. (2007). The maximum θ_e gradient across the upshear eyewall of Claudette (near 1353:40 UTC, Fig. 8a) was ~6 K $\mathrm{km^{-1}}$. The gradient over a broader distance (1353:20–1355:50 UTC), was ~1 K $\mathrm{km^{-1}}$, comparable to the strongest gradients estimated for Hurricane Inez at 700 hPa (~1.7 K $\mathrm{km^{-1}}$; Hawkins and Imbembo 1976) and Hurricane Diana at 850 hPa (~1.4 K $\mathrm{km^{-1}}$; Kossin and Eastin 2001). Given the persistent large shear, it is reasonable to assume that ventilation provided a negative impact throughout the period after hurricane intensity was reached. Prior to rapid intensification, such ventilation was likely of less consequence because of the shallow nature of the vortex. It was only after the vortex intensified and deepened that this process could become important. Direct evidence of ventilation existed near 1530 UTC, just before the storm weakened dramatically. Although this cross-storm flow at 700 hPa does not fit the typical pattern of vertical shear–induced circulation (Marks et al. 1992; Cram et al. 2007), it does suggest that ventilation played a role in the weakening of the storm.

Finally, the entrainment of such dry air into the eyewall and eye could be enhanced by mixing. Kossin and Eastin (2001) have shown that while intensifying, some storms exhibit vorticity and θ_e maxima in the eyewall (their regime 1), but once the storm begins to weaken the vorticity and θ_e maxima shift to a maximum in the center of the eye (their regime 2). Kossin and Eastin (2001) argued that the transition from regime 1 to 2 was due to the extensive mixing that can occur when unstable vorticity gradients within the eyewall break down. The θ_e fields in Claudette appear to show a transition from dual maxima to a single maximum (cf. Figs. 8a and 9a), although the presence of suspected wetting errors in Fig. 9a complicate this interpretation. The vorticity fields (Fig. 10) indicate that the maximum shifted from the eyewall to the center. The center value was larger than the previous eyewall maxima, which could not result from mixing alone. Nevertheless, the shift of the maximum vorticity to the storm center suggests that mixing between the eye and the eyewall did occur in Claudette, and such a process would entrain some of the dry air from upshear (e.g., Kossin and Schubert 2001, their Fig. 10). It is hypothesized that mixing and possibly downdraft cooling occurred in the eyewall of Claudette prior to its weakening. No boundary layer flights are available to evaluate this hypothesis, but it is supported by the dramatic decrease in convection in the core of the storm between 1530 and 1800 UTC (Fig. 5d).

A key question involves the source of the dry air, which was not evident in the prehurricane vortex at 0600 UTC 10 August. A plume of dust and dry air from the Saharan air layer (SAL) existed around the northern and western edges of Claudette throughout the storm's life (J. Dunion 2007, personal communication). The total precipitable water field from the Special Sensor Microwave Imager (SSM/I; not shown), however, showed that this dry air appeared to move westward with the storm, and remained more than 300 km from the storm core.

In situ drying of the air upshear due to vertical wind shear–induced subsidence (Frank and Ritchie 2001) appears to be the most likely source. Evidence of such subsidence is seen upshear near 1200 UTC at 850 hPa (Fig. 7b) as an increase in temperature and a decrease in dewpoint. The shear-induced secondary circulation would be expected to strengthen as the storm intensified. As the vortex deepened in association with the intensification of the system, the depth over which the shear could interact with the vortex increased. Together these could account for the appearance of dry air near the core at 1200 UTC after it was not evident at 0600 UTC. Once the dry air appeared in the lower troposphere, it would have been advected azimuthally by the rapidly intensifying circulation, and could have acted to reduce convection in other quadrants (Molinari et al. 2006). Some evidence of this was provided by the dry air left and right of shear in Fig. 9b. Once dry air was present so close to the center, the various mechanisms noted above provided numerous opportunities to cool the core and produce the observed weakening. By this reasoning, Claudette, even though it was a fully-fledged hurricane at 1200 UTC 10 August, might have been doomed to fail as long as the vertical wind shear remained strong.

c. Summary

Hurricane Claudette provided another example of a storm that developed despite the presence of substantial vertical wind shear. Rapid development occurred as convection shifted to the center of the storm from more than 100 km downshear over a 12-h period. The process differed from the examples presented by Molinari et al. (2004, 2006), in which the center reformed within the downshear convection. The intensification of Claudette also differed from the tropical transition described by Davis and Bosart (2003), in which baroclinic processes played a key role. Nevertheless, these cases show that the mechanism for intensification of tropical cyclones is often strongly tied to the presence of vertical wind shear. Unlike the examples above, Hurricane Claudette weakened as rapidly as it intensified.

Short-lived hurricane vortices likely have occurred in the past but have not been captured until frequent reconnaissance and a key dropsonde revealed this storm. The existence of a fragile, small, but genuinely hurricane-strength vortex at the surface for 6 h presents difficult problems for forecasters. Such a "temporary hurricane" in strongly sheared flow might require a different warning protocol than longer-lasting hurricane vortices in weaker shear.

A number of issues remain unresolved with Hurricane Claudette. It existed within a larger-scale easterly wave, but the exact role of the wave is unclear. The process by which convection was able to move into the center of the storm in the presence of strong shear could not be determined. In a broader sense, a great deal more work is needed to describe how vertical wind shear and dry air act to modulate the intensity of tropical cyclones.

Acknowledgments. We thank Jason Dunion of the HRD of the National Oceanographic and Atmospheric Administration for helping to clarify the role of the SAL in Claudette's evolution, and Dr. Matt Eastin of the University of North Carolina, Charlotte, for providing additional information regarding instrument wetting errors and dry air in hurricanes. We also thank Gareth Berry and three anonymous reviewers for their numerous constructive comments and careful reading of the manuscript. We are much obliged to Dr. John Knaff of the Cooperative Institute for Research in the Atmosphere (CIRA) and Neal Dorst of HRD for maintaining archives of the USAF reconnaissance data, and to Dr. Mark DeMaria (CIRA) for providing the SHIPS shear data. We are indebted to David Vollaro for many of the programs used for shear calculations and analyzing the reconnaissance data. NCEP and ECMWF data were obtained from the National Center for Atmospheric Research, which is supported by the National Science Foundation. This work was supported by NSF Grant ATM0418682 and NASA Grant NNG05GR26G.

REFERENCES

Black, M. L., J. F. Gamache, F. D. Marks Jr., C. E. Samsury, and H. E. Willoughby, 2002: Eastern Pacific Hurricanes Jimena of 1991 and Olivia of 1994: The effect of vertical shear on structure and intensity. *Mon. Wea. Rev.,* **130,** 2291–2312.

Bolton, D., 1980: The computation of equivalent potential temperature. *Mon. Wea. Rev.,* **108,** 1046–1053.

Braun, S. A., and L. Wu, 2007: A numerical study of Hurricane Erin (2001). Part II: Shear and the organization of eyewall vertical motion. *Mon. Wea. Rev.,* **135,** 1179–1194.

——, M. T. Montgomery, and Z. Pu, 2006: High-resolution simulation of Hurricane Bonnie (1998). Part I: The organization of eyewall vertical motion. *J. Atmos. Sci.,* **63,** 19–42.

Chelton, D. B., and F. J. Wentz, 2005: Global microwave satellite observations of sea surface temperature for numerical weather prediction and climate research. *Bull. Amer. Meteor. Soc.,* **86,** 1097–1115.

Chen, S. S., J. A. Knaff, and F. D. Marks Jr., 2006: Effects of vertical wind shear and storm motion on tropical cyclone rainfall asymmetries deduced from TRMM. *Mon. Wea. Rev.,* **134,** 3190–3208.

Corbosiero, K. L., and J. Molinari, 2002: The effects of vertical wind shear on the distribution of convection in tropical cyclones. *Mon. Wea. Rev.,* **130,** 2110–2123.

Cram, T. A., J. Persing, M. T. Montgomery, and S. A. Braun, 2007: A Lagrangian trajectory view on transport and mixing processes between the eye, eyewall, and environment using a high-resolution simulation of Hurricane Bonnie (1998). *J. Atmos. Sci.,* **64,** 1835–1856.

Davis, C. A., and L. F. Bosart, 2003: Baroclinically induced tropical cyclogenesis. *Mon. Wea. Rev.,* **131,** 2730–2747.

——, and ——, 2004: The TT problem: Forecasting the tropical transition of cyclones. *Bull. Amer. Meteor. Soc.,* **85,** 1657–1662.

DeMaria, M., M. Mainelli, L. K. Shay, J. A. Knaff, and J. Kaplan, 2005: Further improvements to the Statistical Hurricane Intensity Prediction Scheme (SHIPS). *Wea. Forecasting,* **20,** 531–543.

Dvorak, V. F., 1984: Tropical Cyclone intensity analysis using satellite data. NOAA Tech. Rep. NESDIS 11, 47 pp. [Available from National Technical Information Service, 5285 Port Royal Rd., Springfield, VA 22161.]

Eastin, M. D., P. G. Black, and W. M. Gray, 2002: Flight-level thermodynamic instrument wetting errors in hurricanes. Part I: Observations. *Mon. Wea. Rev.,* **130,** 825–841.

——, W. M. Gray, and P. G. Black, 2005: Buoyancy of convective vertical motions in the inner core of intense hurricanes. Part I: General statistics. *Mon. Wea. Rev.,* **133,** 188–208.

——, P. D. Reasor, D. S. Nolan, F. D. Marks Jr., and J. F. Gamache, 2006: Evolution of low-wavenumber vorticity during rapid intensification: A dual Doppler analysis. Preprints, *27th Conf. on Hurricanes and Tropical Meteorology,* Monterey, CA, Amer. Meteor. Soc., 4B.6. [Available online at http://ams.confex.com/ams/pdfpapers/108393.pdf.]

Enagonio, J., and M. T. Montgomery, 2001: Tropical cyclogenesis via convectively forced vortex Rossby waves in a shallow water primitive equation model. *J. Atmos. Sci.,* **58,** 685–706.

Frank, W. M., and E. A. Ritchie, 2001: Effects of vertical wind shear on the intensity and structure of numerically simulated hurricanes. *Mon. Wea. Rev.,* **129,** 2249–2269.

Hanley, D., J. Molinari, and D. Keyser, 2001: A composite study of the interactions between tropical cyclones and upper-tropospheric troughs. *Mon. Wea. Rev.,* **129,** 2570–2584.

Hawkins, H. F., and S. M. Imbembo, 1976: The structure of a small, intense hurricane—Inez 1966. *Mon. Wea. Rev.,* **104,** 418–442.

Hendricks, E. A., M. T. Montgomery, and C. A. Davis, 2004: The role of "vortical" hot towers in the formation of Tropical Cyclone Diana (1984). *J. Atmos. Sci.,* **61,** 1209–1232.

Hoffman, R. N., and S. M. Leidner, 2005: An introduction to the near-real-time QuikSCAT data. *Wea. Forecasting,* **20,** 476–493.

Kelley, O. A., J. Stout, and J. B. Halverson, 2004: Tall precipitation cells in tropical cyclone eyewalls are associated with tropical cyclone intensification. *Geophys. Res. Lett.,* **31,** L24112, doi:10.1029/2004GL021616.

Kossin, J. P., and M. D. Eastin, 2001: Two distinct regimes in the kinematic and thermodynamic structure of the hurricane eye and eyewall. *J. Atmos. Sci.,* **58,** 1079–1090.

——, and W. H. Schubert, 2001: Mesovortices, polygonal flow patterns, and rapid pressure falls in hurricane-like vortices. *J. Atmos. Sci.,* **58,** 2196–2209.

Lawrence, M. B., L. A. Avila, J. L. Beven, J. L. Franklin, R. J. Pasch, and S. R. Stewart, 2005: Atlantic hurricane season of 2003. *Mon. Wea. Rev.,* **133,** 1744–1773.

Lungu, T., Ed., 2001: QuikSCAT science data product user's manual: Overview and geophysical data products. JPL D-18053, Version 2.2, Jet Propulsion Laboratory, Pasadena, CA, 95 pp.

Marks, F. D., Jr., R. A. Houze Jr., and S. S. Chen, 1992: Dual-aircraft investigation of the inner core of Hurricane Norbert. Part I: Kinematic structure. *J. Atmos. Sci.,* **49,** 919–942.

Molinari, J., D. Vollaro, and K. L. Corbosiero, 2004: Tropical cyclone formation in a sheared environment: A case study. *J. Atmos. Sci.,* **61,** 2493–2509.

——, P. Dodge, D. Vollaro, K. L. Corbosiero, and F. Marks Jr., 2006: Mesoscale aspects of downshear reformation of a tropical cyclone. *J. Atmos. Sci.,* **63,** 341–354.

Montgomery, M. T., M. E. Nicholls, T. A. Cram, and A. B. Saunders, 2006: A vortical hot tower route to tropical cyclogenesis. *J. Atmos. Sci.,* **63,** 435–465.

Powell, M. D., 1990: Boundary layer structure and dynamics in outer hurricane rainbands. Part II: Downdraft modification and mixed layer recovery. *Mon. Wea. Rev.,* **118,** 918–938.

——, S. H. Houston, L. R. Amat, and N. Morisseau-Leroy, 1998: The HRD real-time hurricane wind analysis system. *J. Wind Eng. Ind. Aerodyn.,* **77–78,** 53–64.

Reasor, P. D., M. T. Montgomery, F. D. Marks Jr., and J. F. Gamache, 2000: Low-wavenumber structure and evolution of the hurricane inner core observed by airborne dual-Doppler radar. *Mon. Wea. Rev.,* **128,** 1653–1680.

Rogers, R., S. Chen, J. Tenerelli, and H. Willoughby, 2003: A numerical study of the impact of vertical shear on the distribution of rainfall in Hurricane Bonnie (1998). *Mon. Wea. Rev.,* **131,** 1577–1599.

Shelton, K. L., 2005: Thermodynamic structure of tropical cyclones from aircraft reconnaissance. M.S. thesis, Dept. of Earth and Atmospheric Sciences, University at Albany, State University of New York, 166 pp.

Simpson, R. H., and H. Riehl, 1958: Mid-tropospheric ventilation as a constraint on hurricane development and maintenance. *Proc. Tech. Conf. on Hurricanes,* Miami, FL, Amer. Meteor. Soc., D4.1–D4.10.

Wong, M. L. M., and J. C. L. Chan, 2004: Tropical cyclone intensity in vertical wind shear. *J. Atmos. Sci.,* **61,** 1859–1876.